ASC24- 5LOr2B-05

Quench Protection of the Fusillo Demonstrator Curved CCT Magnet

M. Wozniak, A. Devred, R. Ferriere, C. Geuzaine, A. Haziot, G. Kirby, E. Ravaioli and A. Verweij

***Abstract*— A quench protection study was performed on the Fusillo Demonstrator Curved Canted Cosine Theta (CCCT) dipole magnet developed at CERN. This magnet features an aperture of 236 mm and a bending radius and angle of 1 m and 90 degrees, respectively. It has an inductance of 9.14 H, a peak winding field of 3.6 T and multi-harmonic aperture field correction. Ten turns of a rope cable made of Nb-Ti strands are placed in each channel of aluminium formers, which are surrounded by an aluminium shell. The aluminium structures not only support mechanical forces but also affect the quench behavior of the magnet. A discharge of the stored energy over an external resistor results in significant eddy current heating of the aluminium structures, which quickly brings a large part of the superconducting winding to the resistive state.**

A three-dimensional (3D) simulation of the eddy currents and heat propagation in the formers with heat propagation in the magnet windings was performed. It uses a cooperative simulation approach involving two software tools developed at CERN as part of the STEAM framework: a finite-element-based tool called FiQuS and a finite-difference-based tool called LEDET. FiQuS calculates the eddy currents and the temperature distribution of the formers, whereas LEDET calculates the current, voltage, and temperature of the windings. This approach enables a 3D quench simulation with great geometrical detail while maintaining reasonable computational cost.

Energy extraction with a fixed resistor is studied, and key parameters of the discharge are calculated. The voltage of the magnet remains below the target specification of 1.5 kV, and the adiabatic hot spot temperature of the windings reaches 185 K. It is shown that the magnet differential inductance and winding resistance dominate the protection transient. The simulations provide great insights into the transient behaviour of the magnet, including the metal structures' temperature and the eddy currents' temporal and spatial distribution.

***Index Terms*— simulations, finite difference methods, finite element method, superconducting magnets, quench protection**

I. Introduction

THE FUSILLO project at CERN is focused on developing technology for Curved Canted Cosine Theta (CCCT) magnets [1], and is an extension of [2]. The Fusillo (technology) Demonstrator uses Nb-Ti strands and its operation at 4.2 K is studied in this contribution. The magnet was designed using CERN simulation tools [3, 4] with a modulation of the winding path required to balance out the field harmonics resulting from the curvature. As a result, magnet windings take elaborate shapes. The practical challenge of winding complex shape coils is reduced by utilizing a so-called rope-cable consisting of twisted and insulated strands connected in series [1].

The magnet has a relatively low operating current and high inductance, and its quench protection is based on active quench detection followed by an energy extraction (EE), which are both available at the CERN magnet test facility. A test campaign of the Fusillo Demonstrator magnet is scheduled for early 2025. The simulation results presented in this paper provide an estimate of the safe powering of the magnet during the tests.

During the EE, very large eddy currents are induced in the aluminium metal structure of the magnet. The magnet differential inductance is affected by the magnetic coupling to the structure, which in turn affects the magnet discharge characteristics. The heat generated by the eddy currents has the potential to quickly quench a large fraction of the windings, a phenomenon called quench back, which is beneficial in quench protection. The magnet's normal state (at 10 K) resistance is several Ω , and a quench of a large part of the winding, with current close to the nominal, can generate a large resistive voltage. In turn, this can have an impact on the magnet quench integral and adiabatic coil's hot spot temperature during quench. The specification maximum voltage between the windings and the formers is 1.5 kV. An adiabatic hot spot temperature limit of 200 K is assumed to be safe for the windings.

A quench simulation of a large CCCT magnet is far from trivial. The shape of the windings and the formers do not allow for the use of symmetry, and 3D simulations are required to account for the eddy currents in a complex metal structure. The metal structure of the Fusillo Demonstrator magnet is on the order of meters and has features such as winding channel ribs and spaces between the formers, which are only a few mm in size. A finite element method is used for the quench simulation, and great care is taken at the geometry, mesh, and solution stages so as not to introduce unnecessary complexity and enable the use of a standard desktop computer for the simulations. Another simulation challenge is that the total length of the magnet conductor, i.e., all the strands connected in series, is about 14 km. A very efficient finite difference approach with a semi-implicit thermal solver is used. The full winding length is discretized, and a 3D heat flow is accounted for with a reasonable computational cost.

The Finite Element Quench Simulator (FiQuS) [5, 6, 7] and Lumped-Element Dynamic Electro-Thermal (LEDET) [8, 9, 10] tools are used for the above tasks. Splitting the simulations across the two tools requires a methodology for coupling the two simulations into a consistent setup and solution. For this, a cooperative simulation (co-simulation) approach is used [11],

M. Wozniak, A. Devred, R. Ferriere, A. Haziot, G. Kirby, E. Ravaioli and A. Verweij are with CERN, Meyrin, Switzerland (e-mail: mariusz.wozniak@cern.ch).

C. Geuzaine is with the University of Liège, 4000 Liège, Belgium.

Manuscript received September 2024.

benefiting from the Python-based co-simulation (PyCoSim) module of the STEAM SDK package [12]. All the software has been developed as part of the STEAM (Simulation of Transient Effects in Accelerator Magnets) framework [13].

The approach has been validated for the quench simulations of the first [14] and second [15] Fusillo Subscale magnets, which are shorter and have fewer channel turns than the Demonstrator but otherwise share almost the same characteristics. However, it is used here for the first time to such a large magnet with a strong quench back, as will be discussed later. For an overview of other recent simulation approaches of straight or curved CCT magnets, see [11].

II. Magnet and Powering Setup

The details of the Fusillo Demonstrator magnet and its specification are given in [1]. Only selected key parameters are shown in Table 1.

TABLE I
KEY PARAMETERS OF THE FUSILLO DEMONSTRATOR [1]

Parameter	Value	Unit
Free aperture	236	mm
Curvature radius	1.0	m
Magnetic bend/length	90 / 1.57	° / m
Nominal current I_{nom}	288	A
Bore/peak field at I_{nom}	3.00 / 3.6	T
Simulated inductance at I_{nom}	9.14	H
# channel turns per layer	65	-
# strands in channel	70	-

Fig. 1 at the top shows the inner and outer windings with the surface color reflecting the strand's magnetic field at a nominal current of 288 A. The peak field of 3.6 T occurs at a location that is characteristic of a CCT magnet.

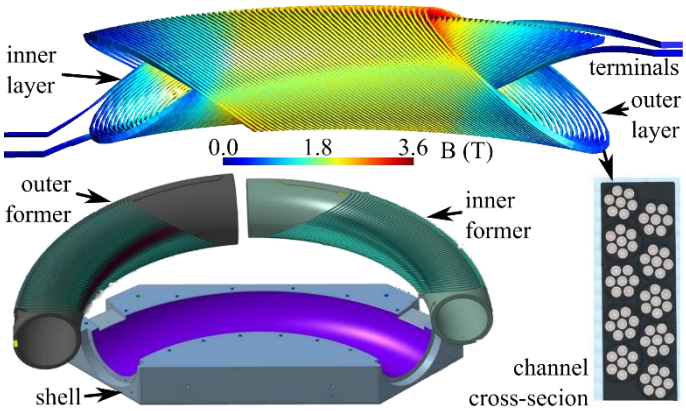

Fig. 1 (top) Magnet windings and their field distribution. (bottom left) View of the main metal elements of the magnet consisting of the inner and outer former and the shell (only the bottom part is shown). (bottom right) Cross-section of the channel with 10 rope cables consisting of 7 strands each.

The bottom part of Fig. 1 shows an exploded view of the main metal elements of the magnet, which are made of an aluminium alloy EN AW-6082 T6. The magnet has 9100 turns, which are distributed into two layers, each with 65 channel turns and 70 strands in a channel. The cross-section of the channel winding is shown in the bottom right part of Fig. 1 and consists of 10 rope cables. Each cable is composed of 6-around-1, round, Nb-Ti/Cu, superconducting (SC) strands with a bare diameter of 825 µm and a Cu:SC ratio of 1.95:1. Strand insulation consists of an extruded layer of thermoplastic polyimide. Additional glass fibre braid cable insulation is added, and the winding is impregnated with resin. All the strands are electrically connected in series by resistive splices [1].

The quench was simulated with the magnet being part of the electrical circuit, including PC and EE (Fig. 2). At a nominal current of 288 A, an active quench detection system is assumed to detect a quench in 10 ms. The discharge simulation starts at time t = 0 s by changing the state of the power converter (PC) output stage to a high impedance and opening the energy extraction switch. This results in the magnet current commuting to the PC's internal crowbar resistor of 50 mΩ, the crowbar diode with a voltage of 0.75 V and the EE resistor of 3.422 Ω, all connected in series. This is equivalent to a 1 kV EE at a nominal current of 288 A. The magnet is operated at 4.2 K.

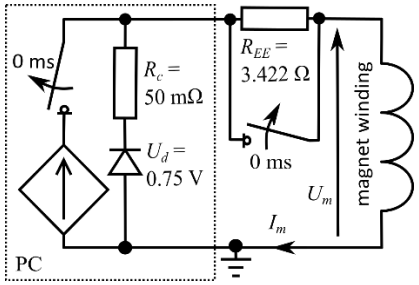

Fig. 2 Schematic of the magnet circuit including power converter (PC) and energy extraction system.

III. Simulation Setup

The FiQuS and LEDET tools are used in the co-simulation, with the Python-based STEAM SDK package [12] maintaining and controlling communication, data exchange, and convergence as described in [11]. It involves initial solutions of parts of the problem in FiQuS and LEDET, followed by iterations involving both tools until the results are within a specified convergence tolerance ε. FiQuS calculated the eddy currents and the temperature distribution in the formers, as well as the magnetic field distribution and differential inductance. LEDET calculated the current, voltage, resistance and temperature in the windings. The simulation results have been validated and agree well with the measurements of the first [14] and the second [15] Fusillo subscale magnets. The key model inputs are reported in [1], whereas some have been refined using the measured data [15].

All the input files required to perform the simulations presented here are available [16].

A. Finite Element tool

The open-source FiQuS tool is coded in Python [17] and, with the help of Gmsh [18, 19] and GetDP [20, 21], performs geometry generation, meshing, solving, and postprocessing.

The magnet geometry enters the simulations as conductor files [22] for winding and STEP files [23] for the formers and

shell. A cylindrical air region of 2 m in diameter and 3 m in length was added around the magnet. The winding terminals are taken into account until the flat ends of the cylindrical air region (see top of Fig. 1).

Crucially for the mesh size and solution time, the thin air gaps between the metal structures and around the windings are collapsed into surfaces (shells), following the approach described in [11]. For this, a series of geometry-level Boolean operations between the winding and the metal structures is needed. An update of Gmsh was required to obtain a conformal geometry in a reasonable time. In version 4.13.0, a feature was introduced that allows the final fragment operation to be performed without checking for an intersection of the volumes, which is not required as the operations are coded such that previous Boolean operations ensure no overlap.

The collapsed-air-gaps conformal geometry greatly simplifies the meshing of the model. The mesh used in the simulations included 1.7M and 1M tetrahedra for the regions used in the magnetoquasistatic and thermal calculations, respectively.

The finite element solution consists of a magnetostatic solution at the initial magnet current, followed by Galerkin projection [24] of magnetic flux as an initial solution for the transient electromagnetic solution. This is followed by sequentially solving coupled electromagnetic and thermal models with volumetric Joule power density from the electromagnetic problem and temperature from the thermal problem exchanged between the solutions. The weak formulations are non-standard and include electrical insulation between the model elements and a controlled thermal connection across the shells. This is achieved by introducing a discontinuous contribution of the magnetic vector potential [25] and using the thin shell approximation [26], respectively [11]. The transient electromagnetic and thermal problems have 2.2M and 1.7M degrees of freedom, and the solution time on a modern desktop computer is about 6 h for computing, on average across co-simulation iterations, 27 adaptive time steps for a 2.5 s transient.

B. Finite Difference Tool

LEDET is coded in MATLAB [27] with a semi-implicit transient thermal solver that accounts for 3D heat diffusion inside the winding as well as Joule heating and Inter-Filament Coupling Loss (IFCL) [8, 9].

The twisted rope cable strands are simulated as straight elements. The polyimide strand insulation and the glass fibre cable are accounted for. Appropriate thermal connections were specified to capture the complex heat exchange patterns between the strands in the cable and between the cables and the formers. These thermal connections use equivalent thicknesses and series connections of insulation layers. The thermal diffusion between the windings and the formers was deduced based on experimental evidence, as described in [15]. The discretization of the full winding results in 1.4M volumes with a solution time of about 7 h for a 2.5 s transient comprising 391 fixed (but not equal) time steps.

IV. Results and Discussion

An energy extraction using a fixed resistance is studied. Section IV.A describes the key characteristics of the discharge, such as magnet voltage, current, differential inductance and winding resistance. Section IV.B focuses on the magnet quench integral and the adiabatic hot spot temperature estimation. This is followed by section IV.C, which describes the temporal and spatial distribution of the eddy current and the temperature of the magnet metal structure. Finally, co-simulation computational efficiency is stated and discussed in section IV.D.

A. Discharge characteristics and key circuit elements

The magnet current and resistive, inductive and total (terminals) voltage are shown in Fig. 3 for a current discharge from 288 A.

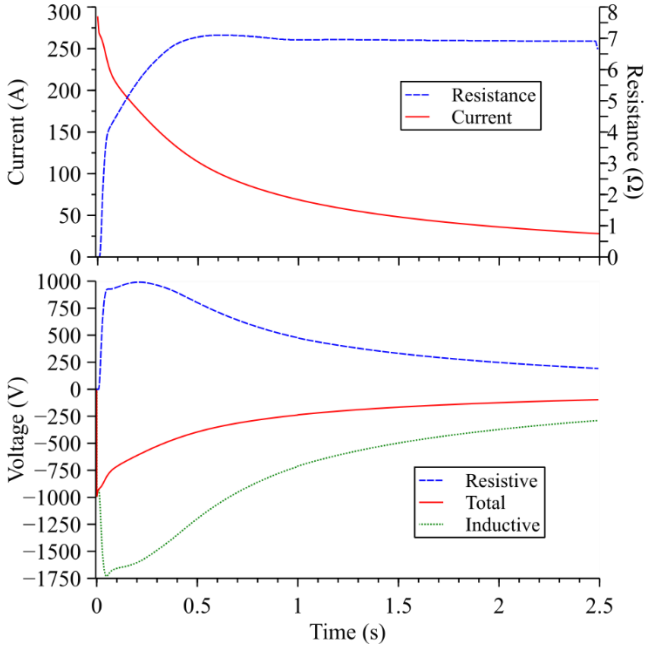

Fig. 3 Evolution of (top) the magnet current and winding resistance, (bottom) the magnet total (terminals) voltage and its inductive and resistive parts.

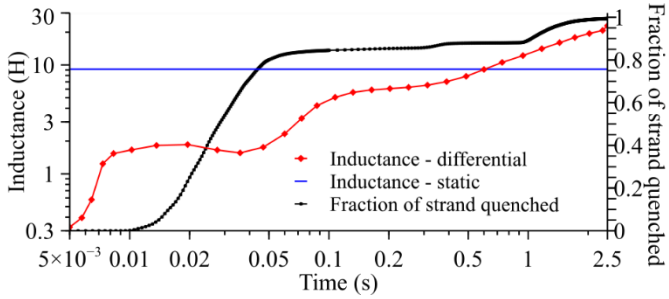

Fig. 4 (left axis) Differential magnet inductance versus time at the time of the 36 adaptive steps of the FiQuS solution. The static magnet inductance is plotted for comparison. (right axis) Fraction of quenched strand versus time, at time steps of the LEDET solution.

The initial current decay to about 260 A is very fast due to a drastically reduced magnet differential inductance, which is plotted vs time in Fig. 4. The differential inductance is about 0.3 H at the first step of the transient solution and increases

later in the transient, even above the static inductance of 9.14 H. The induced eddy currents in the formers and the shell are responsible for this effect. The reduction of the inductance is very beneficial for quench protection as it increases the current decay rate, particularly at the beginning of the transient when the current is maximum. Later in the transient, the energy stored in the eddy currents is partially extracted via magnet terminals, requiring a higher voltage for a given decrease in a magnet current, as compared to a case when the eddy currents would not be present. This effect causes an inductance increase above the static one at times > 0.6 s.

Another consequence of the eddy currents is a dissipation of heat in the metal structures. This heat quickly propagates to the magnet winding, as can be observed by the fraction of the quenched (i.e. with a temperature above the current sharing temperature) strand over time, as plotted in Fig. 4. The winding starts to quench at 10 ms, and more than 80% of it is quenched at 50 ms by the heat generated in the formers and diffused via the insulation.

Fig. 5 shows the temperature distribution of the windings at 37 ms. The winding starts to quench on the sides of the formers, which corresponds to the location where the formers heat up the most, as discussed later. Note that the quench does not start at the high-field region, as some simplified approaches, including STEAM-ProteCCT [28] suggest [29].

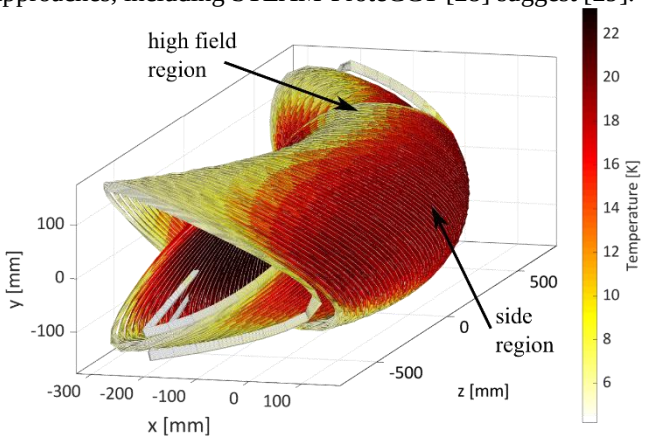

Fig. 5 Magnet windings temperature distribution at time 37 ms.

The quench of a large part of the winding, namely 80% at 50 ms, results in about 4 Ω of winding resistance (see the top part of Fig. 3), which is slightly larger than the energy extraction resistance. Hence, the discharge rate more than doubles, resulting in a large increase in the inductive component of the winding voltage (see the bottom part of Fig. 3). The inductive component balances the resistive component, and the sum equals the terminals voltage. The maximum voltage between the windings and the formers is equal to the voltage of the energy extraction of 1 kV at the beginning of the discharge. This is below the maximum voltage maximum voltage of the magnet specification of 1.5 kV.

B. Adiabatic hot spot temperature

The integration of the square of the magnet current over time results in a quench integral (QI) of 23 kA²s. Assuming 10 ms for detection at 288 A adds 0.8 kA²s detection QI. For the Nb-Ti strand, this total QI of 23.8 kA²s corresponds to the adiabatic winding hot spot temperature of 185 K (see Fig. 6), which meets the requirement of 200 K, and the magnet is considered protected.

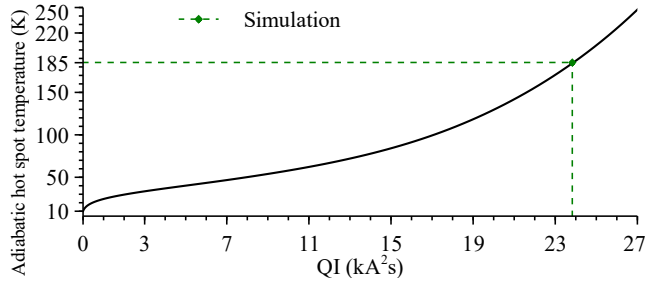

Fig. 6 Calculated adiabatic hotspot temperature for the magnet wire (assuming RRR of the copper of 150) vs current quench integral, QI.

C. Key results distribution in the metal elements

The simulations provide insights into magnet behaviour that would be very difficult to measure, for example, how the total power dissipated in, and the maximum temperature of the metal elements evolve in time, as plotted in Fig. 7.

For the formers, the initial value of about 5-10 kW is due to the energy extraction resistance. The power reaches a peak value of about 30-35 kW at a time of 0.075 s, which follows the quench of the winding. The power in the shell reaches a much higher peak of about 62 kW due to its larger size and cross-section for the current flow. The eddy current time constant in the shell is much longer, with the peak power delayed to about 0.6 seconds.

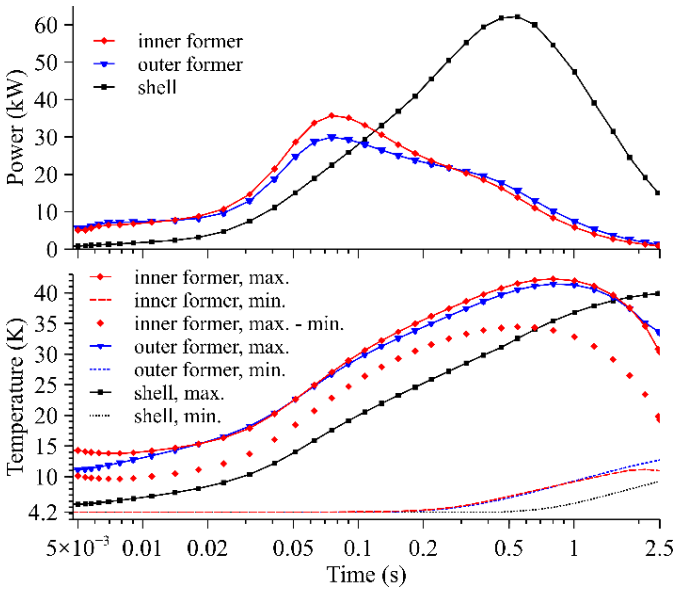

Fig. 7 Evolution in time of the: (top) total power dissipated in, (bottom) maximum temperature of, the metal elements of the magnet structure. At the bottom plot, the minimum temperatures for all and the maximum temperature difference for the inner former are plotted.

The bottom part of Fig. 7 shows the temperature of the metal parts. The maximum temperature of the formers, of about 40 K, is reached at about 1 s into the discharge. Due to the non-uniform power deposition into the formers, the

temperature distribution is non-uniform, and some parts of the structure remain at 0.2 s at the initial temperature. This gives a maximum temperature difference of about 35 K, which is reached at 0.55 s. Lastly, the maximum temperature starts to decrease after about 1 s in the discharge as the heating decreases, and the heat diffusion and cooling begin to dominate the distribution.

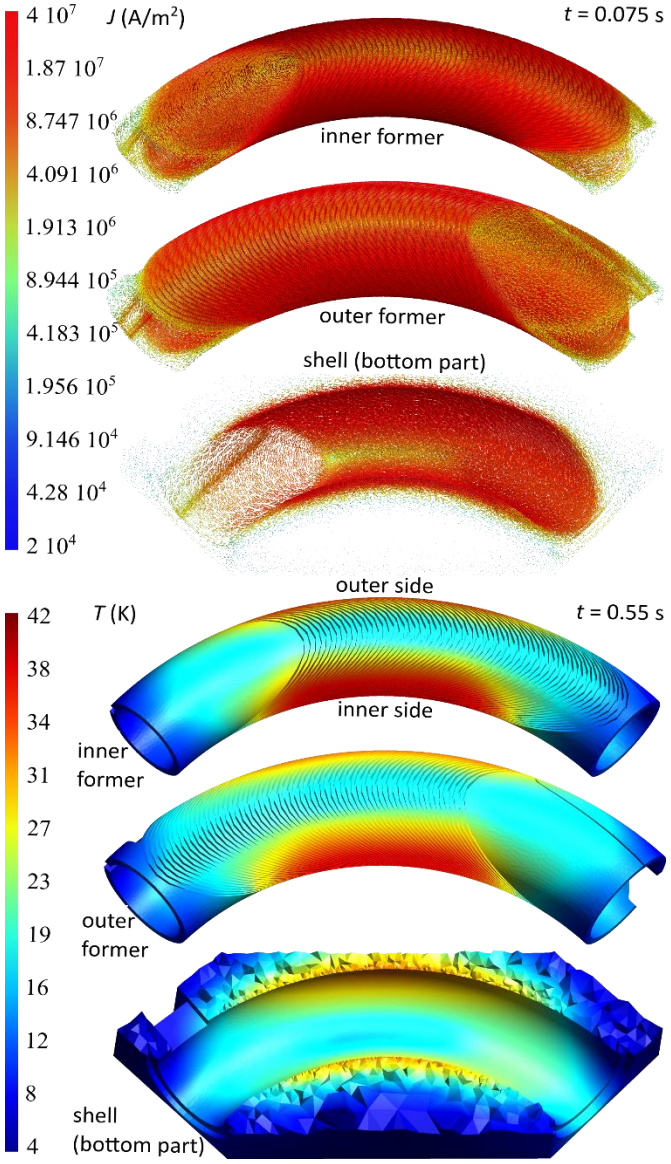

Fig. 8 (top) Eddy current density at t =0.075 s (at a peak as in Fig. 7) and (bottom) temperature at t = 0.55 s (at a peak gradient as in Fig. 7). Eddy current density is shown with arrows to visualize the current flow direction. The formers are shown with the same scale. The shell is shown as smaller compared to the formers, and only the bottom part is shown to improve the visibility of the results.

The simulation results also allow visualization of the distribution of the eddy current density and the temperature. This is presented in Fig. 8 at t = 0.075 s and t = 0.55 s, corresponding to the mentioned peak value and peak difference for the power and temperature, respectively. It should be noted that for this dipole magnet, the eddy currents do not follow a saddle coil-like pattern [29] but flow in a tilted way similar to the windings. The shape corresponds to the induced electromotive force and is affected by the metal cross-section, in particular, by the channels machined in the former. The eddy current density is slightly higher at the inner side of the curved formers and decreases towards the top and bottom of the tube, simply due to geometrical effects (larger apparent cross-section of metal perpendicular to the current flow direction).

The temperature distribution caused by the Joule heating of the eddy currents reaches a maximum above 40 K on both sides of the formers. The inner side of the curved formers has a temperature of about 3 K higher than the outer side due to the curvature of the former, resulting in higher current density inside that region of the curvature.

D. Co-simulaiton numerical performance

The full 3D approach is used with a total co-simulation time on a typical desktop computer of about 93 h (~4 days), and 7 iterations were sufficient for the co-simulation to converge with a criterion based on the magnet current, i.e., $\forall t$: $|I_{\text{iter.N}}(t) - I_{\text{iter.N-1}}(t)| < 2.0$ A. For LEDET, a speed-up could be achieved by using an adaptive time-stepping scheme. At nominal magnet current, most of the winding quenches almost instantaneously. In this case, careful homogenization of the winding in the channel, instead of resolving each strand, might lead to large speed improvements, which remains a topic of future work.

V. Conclusion

The recently developed co-simulation between the finite elements and finite difference tools of the STEAM framework has been used to simulate quench in the Fusillo Demonstrator Curved Canted Cosine Theta (CCCT) magnet. The simulation was able to capture the eddy currents induced in the aluminium metal structure of the magnet and their impact on the magnet differential inductance, which in turn affects the magnet discharge characteristic. The heat generated by the eddy currents very quickly quenched a large fraction of the windings, a phenomenon called quench back. The thermal diffusion in the windings and the resulting large increase in the winding temperature and resistance were also captured by the simulations.

The three-dimensional simulation provides valuable insights into the quench behavior of the CCCT magnets, particularly their eddy current patterns and formers' temperature distribution. The curvature of the magnet results in an increased temperature on the inner side of the bend compared to the outer side. The large temperature difference in the formers highlights the non-uniform temperature distribution. If the temperature of the formers is to be measured, a careful placement of the instrumentation is required.

The initial simulation shows that the voltages to the ground of the magnet do not exceed 1 kV, which is imposed by the energy extraction system used for protection. The peak adiabatic hot spot temperature of 185 K offers a safe temperature margin for protection.

The measurement campaign of the magnet is soon to start, and the comparison between measurements and simulations will be presented in a future paper.

REFERENCES

[1] A. Haziot, A. Dallocchio, A. Devred, A. Foussat, L. Gentini,G. Kirby, F. J. Mangiarotti, M. Pentella, C. Petrone, F.-O. Pincot, J.-S. Rigaud, and J. G.-Valenzuela, "Curved-Canted-Cosine-Theta (CCCT) Dipole Prototype Development at CERN," *IEEE Trans. Appl. Supercond.* Submitted in Sep 2023 in proceedings of the Magnet Technology Conference (MT-28).

[2] G. Kirby, V. Rodin, O. Kirby, A. Foussat, J. Resta-Lopez, I. Martel, and C. Welsch, "Superconducting Curved Canted–Cosine–Theta (CCT) for the HIE-ISOLDE Recoil Separator Ring at CERN, " *IEEE Trans. Appl. Supercond.*, vol. 32, no. 6, Mar 2022, art. no. 4004105. doi: 10.1109/TASC.2022.3158332

[3] ROXIE Users Workshop and ROXIE23 Launch. [Online]. Available: https://indico.cern.ch/event/1318061/

[4] M. Liebsch, S. Russenschuck, "A CAD Engine Based on the Differential Geometry of the Frenet Frame," *IEEE Trans. Appl. Supercond.* Submitted in Sep 2023 in proceedings of Magnet Technology Conference (MT-28).

[5] A. Vitrano , M. Wozniak, E. Schnaubelt, T. Mulder, E. Ravaioli, and A. Verweij, "An Open-Source Finite Element Quench Simulation Tool for Superconducting Magnets," *IEEE Trans. Appl. Supercond.*, vol. 33, no. 5, Aug 2023, art. no. 4702006. doi: 10.1109/TASC.2023.3259332

[6] M. Wozniak, E. Ravaioli, and A. Verweij, "Fast Quench Propagation Conductor for Protecting Canted Cos-Theta Magnets," *IEEE Trans. Appl. Supercond.*, vol. 33, no. 5, Aug 2023, art. no. 4701705, doi: 10.1109/TASC.2023.3247997

[7] STEAM FiQuS. [Online]. Available: https://cern.ch//fiqus

[8] E. Ravaioli, B. Auchmann, M. Maciejewski, H. ten Kate, and A. Verweij, "Lumped-element dynamic electro-thermal model of a superconducting magnet," *Cryogenics*, vol. 80, part 3, Dec 2016, pp. 346-356. doi: 10.1016/j.cryogenics.2016.04.004

[9] E. Ravaioli, O. Tranum Arnegaard, A. Verweij, and M. Wozniak, "Quench Transient Simulation in a Self-Protected Magnet With a 3-D Finite-Difference Scheme," *IEEE Trans. Appl. Supercond.*, vol. 32, no. 6, Sep 2022, art. no. 4005205, doi: 10.1109/TASC.2022.3162798

[10] STEAM LEDET. [Online]. Available: https://cern.ch//ledet

[11] M. Wozniak, E. Schnaubelt, J. Dular, E. Ravaioli, and A. Verweij, "Quench Co-Simulation of Canted Cos-Theta Magnets," *IEEE Trans. Appl. Supercond.* vol. 34, no. 3, Dec 2023, art. no. 3338142, doi: 10.1109/TASC.2023.3338142

[12] STEAM SDK. [Online]. Available: https://pypi.org/project/steam-sdk/

[13] STEAM Framework. [Online]. Available: https://cern.ch//steam

[14] M. Wozniak et al., "Quench Protection of Fusillo Subscale Curved CCT Magnet," *IEEE Trans. Appl. Supercond.*, vol. 34, no. 5, pp. 1-5, Aug 2024, art no. 4702805, doi: 10.1109/TASC.2024.3355358

[15] M. Wozniak et al., " Transient behavior of the Second Fusillo Subscale Curved CCT Magnet,". Submitted in Sep 2024 *IEEE Trans. Appl. Supercond.*, in proceedings of ASC24 conference.

[16] STEAM Analysis Fusillo Demo COSIM GitLab Repository. [Online]. Available: https://gitlab.cern.ch/steam/analyses/fusillo_demo_cosim

[17] Python Programming Language. [Online]. Available: https://www.python.org/

[18] Gmsh. [website]. Available: http://gmsh.info/

[19] C. Geuzaine and J.-F. Remacle, "Gmsh: A 3-D finite element mesh generator with built-in pre- and post- processing facilities," *International Journal for Numerical Methods in Engineering*, vol. 79, pp. 1309–1331, May 2009. doi: 10.1002/nme.2579

[20] GetDP [website]. Available: http://getdp.info/

[21] P. Dular, C. Geuzaine, F. Henrotte, and W. Legros, "A general environment for the treatment of discrete problems and its application to the finite element method," *IEEE Transactions on Magnetics*, vol. 34, no. 5, pp. 3395–3398, 1998. doi: 10.1109/20.717799

[22] Opera Simulation Software [website]. Available: https://www.3ds.com/products-services/simulia/products/opera/

[23] Standard for the Exchange of Product Model data (STEP), ISO-10303-21. [Online]. Available: https://www.iso.org/standard/63141.html

[24] G. Parent, P. Dular, J.-P. Ducreux, and F. Piriou, "Using a Galerkin Projection Method for Coupled Problems," *IEEE Transactions on Magnetics*, vol. 44, no. 6, pp. 830–833, 2008. doi: 10.1109/TMAG.2008.915798

[25] P. Dular and C. Geuzaine, "Modeling of thin insulating layers with dual 3-D magnetodynamic formulations," *IEEE Trans. Magn.*, vol. 39, no. 3, pp. 1139–1142, May 2003, doi: 10.1109/TMAG.2003.810387

[26] E. Schnaubelt, M.Wozniak, and S. Schöps, "Thermal thin shell approximation towards finite element quench simulation," *Supercond. Sci. Technol.*, vol. 36, no. 4, Mar. 2023, Art. no. 044004, doi: 10.1088/1361-6668/acbeea.

[27] MATLAB. [Online]. Available: https://www.mathworks.com/products/matlab.html

[28] STEAM ProteCCT. [Online]. Available: https://cern.ch//protecct

[29] M. Mentink, J. van Nugteren, F. Mangiarotti, M. Duda, and G. Kirby, "Quench Behavior of the HL-LHC Twin Aperture Orbit Correctors," *IEEE Trans. Appl. Supercond.*, Vol. 28, No. 3, 4004806, Apr. 2018, doi: 10.1109/TASC.2018.2794451